Anchored boundary conditions for locally isostatic networks

Louis Theran[*]
Aalto Science Institute and Department of Computer Science, Aalto University, Post Office Box 15500, 00076 Aalto, Finland

Anthony Nixon[†]
Department of Mathematics and Statistics, Lancaster University, Lancaster LA1 4YF, England, United Kingdom

Elissa Ross[‡]
MESH Consultants, Inc., Fields Institute for Research in the Mathematical Sciences, 222 College Street, Toronto, Ontario, Canada M5T 3J1

Mahdi Sadjadi[§]
Department of Physics, Arizona State University, Tempe, Arizona 85287-1504, USA

Brigitte Servatius[‖]
Department of Mathematical Sciences, Worcester Polytechnic Institute, 100 Institute Road, Worcester, Massachusetts 01609, USA

M. F. Thorpe[¶]
Department of Physics, Arizona State University, Tempe, Arizona 85287-1504, USA
and Rudolf Peierls Centre for Theoretical Physics, University of Oxford, 1 Keble Road, Oxford OX1 3NP, England, United Kingdom
(Received 5 August 2015; published 30 November 2015)

Finite pieces of locally isostatic networks have a large number of floppy modes because of missing constraints at the surface. Here we show that by imposing suitable boundary conditions at the surface the network can be rendered *effectively isostatic*. We refer to these as *anchored boundary conditions*. An important example is formed by a two-dimensional network of corner sharing triangles, which is the focus of this paper. Another way of rendering such networks isostatic is by adding an external wire along which all unpinned vertices can slide (*sliding boundary conditions*). This approach also allows for the incorporation of boundaries associated with internal *holes* and complex sample geometries, which are illustrated with examples. The recent synthesis of bilayers of vitreous silica has provided impetus for this work. Experimental results from the imaging of finite pieces at the atomic level need such boundary conditions, if the observed structure is to be computer refined so that the interior atoms have the perception of being in an infinite isostatic environment.

DOI: 10.1103/PhysRevE.92.053306 PACS number(s): 46.15.−x, 63.50.Lm

I. INTRODUCTION

Boundary conditions are paramount in many areas of computer modeling in science. At the atomic level, finite samples require appropriate boundary conditions in order that atoms in the interior behave as if they were part of a larger or infinite sample, or as closely to this as is possible. One example of this is the calculation of the electronic properties of covalent materials where the surface is terminated with H atoms so that all the chemical valency is satisfied. In this way the highest occupied molecular orbital and the lowest unoccupied molecular orbital states inside the sample can be obtained and are not very different from those expected in the bulk sample. In materials science, the electronic band structure of a sample of crystalline Si could be obtained by determining the electronic properties of a finite cluster terminated with H bonds at the surface. In practice this is rarely done, as it is more convenient to use periodic boundary conditions and, hence, use Bloch's Theorem, but this technique has been used recently in graphene nanoribbons [1].

For most samples, the nature of the boundary—fixed, free, or periodic—only alters the properties of the sample by the ratio of the number of atoms on the surface to those in the bulk. This ratio is $N^{-\frac{1}{d}}$ where N is the number of atoms (later referred to as vertices) and d is the dimension. Of course this ratio goes to zero in the thermodynamic limit as the size of the system $N \to \infty$ and leads to the important result that properties become independent of boundary conditions for large enough systems.

Similar statements can be made about the mechanical and vibrational properties of systems *except* for isostatic networks that lie on the border of mechanical instability. In this case the boundary conditions are important no matter how large N, and special care must be taken with devising boundary conditions so that the interior atoms behave as if they were part of an infinite sample, in as much as this is possible [2–4].

In Fig. 1, we show a part of a scanning probe microscope (SPM) image [5] of a bilayer of vitreous silica which has the chemical formula SiO_2. The sample consists of an upper layer of tetrahedra with all the apexes pointing downwards where they join a mirror image in the lower layer. In the figure we show the triangular faces of the upper tetrahedra, which form

[*]louis.theran@aalto.fi; http://theran.lt
[†]a.nixon@lancaster.ac.uk; http://www.lancaster.ac.uk/maths/about-us/people/anthony-nixon
[‡]elissa.ross@meshconsultants.ca; http://www.elissaross.ca
[§]ssadjadi@asu.edu
[‖]bservat@wpi.edu; http://users.wpi.edu/∼bservat
[¶]mft@asu.edu; http://thorpe2.la.asu.edu/thorpe

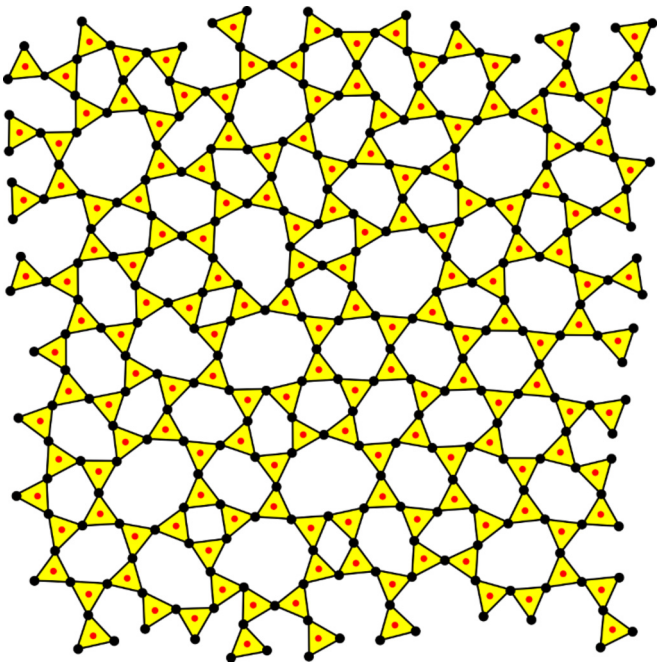

FIG. 1. (Color online) A piece of bilayer of vitreous silica derived from an SPM image [5]. The Si atoms are shown as red discs (in the centers of triangles) and the O atoms (corners of triangles) as black discs. The local covalent bonding leads to the yellow almost-equilateral triangles that are freely jointed, which we will refer to as *pinned*. The triangles at the surface have either one or two vertices unpinned.

rigid triangles with a (red) Si atom at the center and the (black) O atoms at the vertices of the triangles which are freely jointed to a good approximation. We refer to these networks as *locally isostatic* as the number of degrees of freedom of the equilateral triangle in two dimensions is exactly balanced by the shared pinning constraints (two at each of the three vertices, so that $3 - 2 \times 3/2 = 0$). While the three-dimensional bilayers are locally isostatic, so too are the two-dimensional (2D) projections of corner-sharing triangles which are the focus of this paper. We will use the *Berlin A* sample as the example throughout [6,7] so that we can focus on this single geometry for pedagogical purposes.

Because experimental samples are always finite in extent and usually have irregular boundaries, including internal regions that are either absent or not imaged, it is necessary to develop appropriate boundary conditions. Note that the option of cutting a rectangular piece out of the experimental image is not available because of the amorphous nature of the network, which means that it is not possible for the left side to connect to the right side as with a regular crystalline network. Even if this were possible, it would be unwise to discard experimental data and hence lose information. In this paper we show how boundary conditions can be applied to locally isostatic systems which are not periodic.

We show rigorously that there are various ways to add back the exact number of missing constraints at the surface, sufficiently uniformly distributed around the boundary, that the network is guaranteed to be isostatic everywhere. There is some limited freedom in the precise way these boundary conditions are implemented, and the boundary can be general enough to include internal holes. The proof techniques used here involve showing that *all* subgraphs have insufficient edge density for redundancy to occur [8]. In the Appendix, we give an algorithmic description of our boundary conditions and discuss in detail how to ensure the resulting boundary is sufficiently generic.

Using the pebble game [9,10], we verified on a number of samples that anchored boundary conditions in which alternating free vertices are pinned result in a global isostatic state. The pebble game is a combinatorial (integer) algorithm, based on Laman's theorem [8], which for a particular network performs a rigid region decomposition. This involves finding the rigid regions, the hinges between them, and the number of floppy (zero-frequency) modes. We have used it to confirm that the locally isostatic samples such as that in this paper are isostatic overall with anchored boundary conditions. The results of this paper imply that, under a relatively mild connectivity hypothesis, this procedure is provably correct and thus relatively robust. Additionally, the necessity of running the pebble game for each individual case is avoided.

Figure 2 shows *sliding* boundary conditions [12]. These make use of a different, simpler kind of geometric constraint at each unpinned surface site. The global effect on the network's degrees of freedom is like that of the anchored boundary conditions, and this setup is computationally reasonable. At the

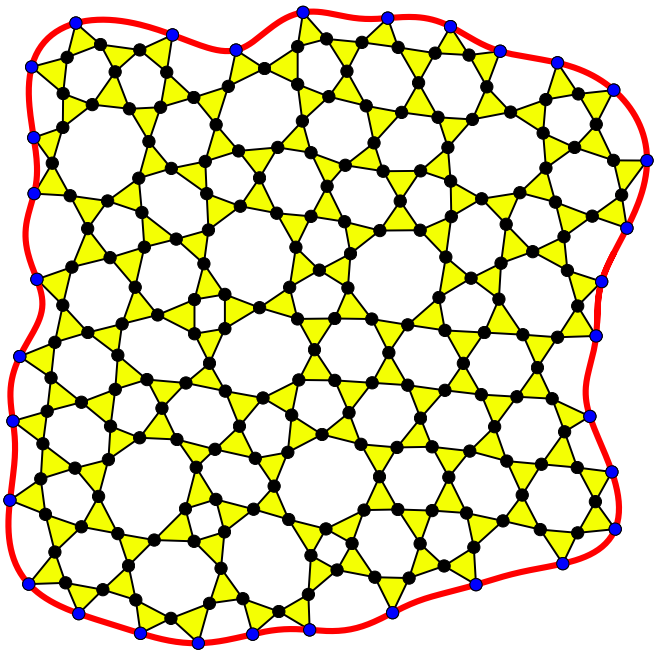

FIG. 2. (Color online) Sliding boundary conditions, used for a piece of the sample shown in Fig. 1. The boundary sites are shown as blue discs and the three purple triangles at the lower right in Fig. 3 have been removed. The red Si atoms at the centers of the triangles in Fig. 1 have also been removed for clarity. The boundary is formed as a smooth analytic curve by using a Fourier series with 16 sine and 16 cosine terms to match the number of surface vertices, where the center for the radius $r(\theta)$ is placed at the centroid of the 32 boundary vertices [11]. Note that sliding boundary conditions do not require an even number of boundary sites.

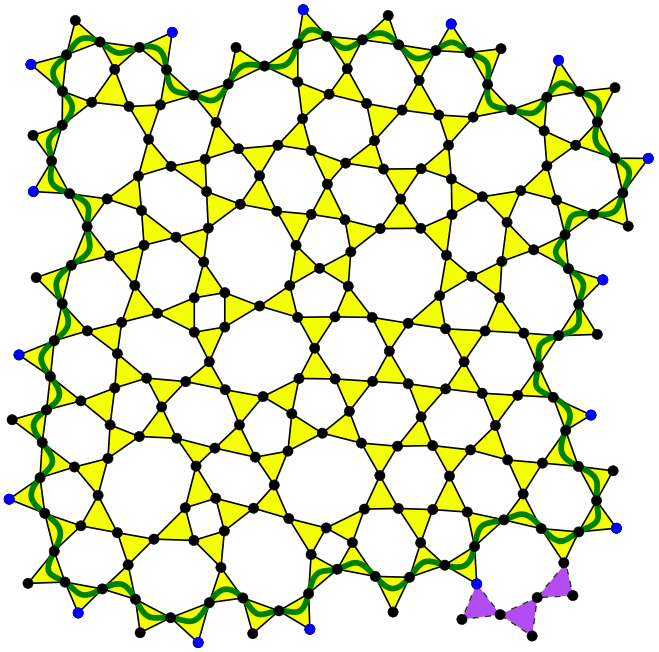

FIG. 3. (Color online) The anchored boundary conditions used for the sample shown in Fig. 1. The alternating anchored sites on the boundary are shown as blue discs and the three purple triangles at the lower right are removed to give an even number of unpinned surface sites. The red Si atoms at the centers of the triangles in Fig. 1 have been suppressed for clarity.

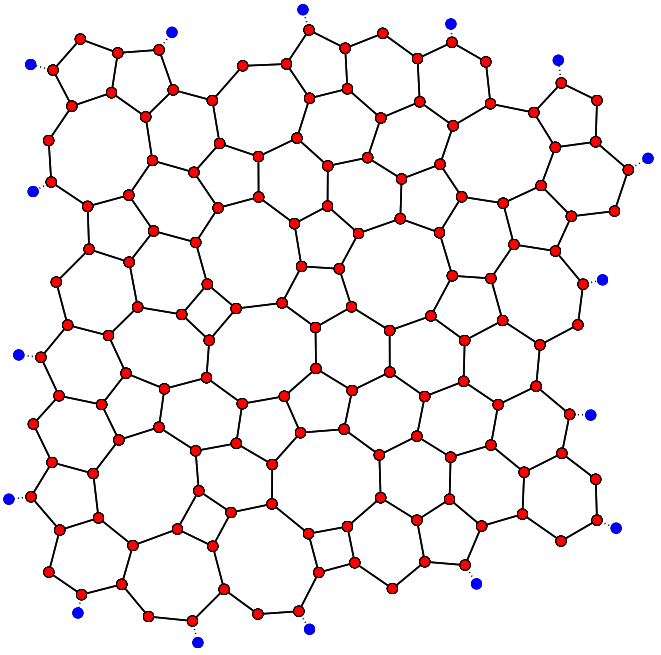

FIG. 4. (Color online) The triangle ring network, complementary to that in Fig. 3, where the Si atoms, shown as red discs, at the center of each triangle are emphasized in this three-coordinated network. Dashed edges are shown connecting to the anchored sites.

same time, the proofs for this case are simpler, and generalize more easily to handle situations such as holes in the sample.

In Fig. 3, we show the anchored boundary conditions. We have trimmed off the surface triangles in Fig. 1 that are only pinned at one vertex. This makes for a a more compact structure whose properties are more likely to mimic those of a larger sample, and makes our mathematical statements easier to formulate. In addition we have had to remove the three purple triangles at the lower right-hand side in order to get an even number of unpinned surface sites. When the network is embedded in the plane, this is possible, except for very degenerate samples (see Fig. 3).

II. COMBINATORIAL ANCHORING

Intuitively, the internal degrees of freedom of systems like the ones in Figs. 1 and 3 correspond to the corners of triangles that are not shared. This is, in essence, the content of Lemma 1 proved below. Proving Lemma 1 requires ruling out the appearance of *additional* degrees of freedom that could arise from *substructures* that contain more constraints than degrees of freedom.

The essential idea behind combinatorial rigidity [13] is that *generically* all geometric constraints are visible from the topology of the structure, as typified by Laman's [8] striking result showing the sufficiency of Maxwell counting [15] in dimension 2. Genericity means, roughly, that there is no special geometry present; in particular, generic instances of any topology are dense in the set of all instances.

In what follows, *we will be assuming genericity*, and then use results similar to Laman's, in that they are based on an appropriate variation of Maxwell counting. Our proofs have a graph-theoretic flavor, which relate certain hypotheses about connectivity [16] to hereditary Maxwell-type counts.

A. Triangle ring networks

We will model the flexibility in the upper layer of vitreous silica bilayers as systems of 2D triangles, pinned together at the corners. The joints at the corners are allowed to rotate freely. These are examples of body-pin networks [18] from rigidity theory. A body-pin network is *rigid* if the only available motions preserving triangle shapes and the network's connectivity are rigid body motions; it is *isostatic* if it is rigid, but ceases to be so once any joint is removed.

The combinatorial model is a graph G that has one vertex for each triangle and an edge between two triangles if they share a corner (Fig. 4). Since we are assuming genericity, we will identify a geometric realization with the graph G from now on. In what follows, we are interested in a particular class of graphs G, which we call *triangle ring networks*. The definition of a triangle ring is as follows: (a) G has only vertices of degree 2 and 3; G is 2-connected [23]; (b) there is a simple cycle C in G that contains all the degree 2 vertices, and there are at least three degree 2 vertices; (c) any edge cut set [24] in G that disconnects a subgraph containing only degree 3 vertices has size at least 3.

To set up some terminology, we call the degree 2 vertices *boundary vertices* and the degree 3 vertices *interior vertices*. A subgraph spanning only interior vertices is an *interior subgraph*.

The reader will want to keep in mind the specific case in which G is planar with a given topological embedding and C is the outer face, as is usually the case in our figures. This means that subgraphs strictly interior to the outer face have only

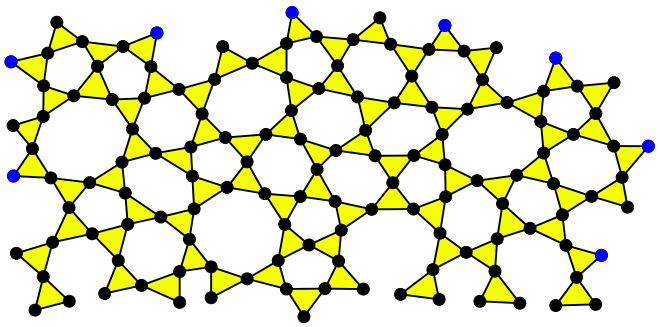

FIG. 5. (Color online) A typical subgraph from Fig. 3 used in the proof that there are no rigid subgraphs larger than a single triangle. (See Lemma 1.)

interior vertices, which explains our terminology. However, as we will discuss in detail later, the setup is very general. If the sample has holes, C can leave the outer boundary and return to it: provided that it is simple, all the results here still apply.

A theorem of Tay-Whiteley [19,20] gives the degree of freedom counts for networks of two-dimensional bodies pinned together. Generically, there are no stressed subgraphs in such a network, with graph G, of v bodies and e pins if and only if

$$2e' \leqslant 3v' - 3 \qquad \text{for all subgraphs } G' \subset G, \tag{1}$$

where v' and e' are the number of vertices and edges of the subgraph. If Eq. (1) holds for all subgraphs, the rigid subgraphs are all isostatic, and they are the subgraphs where Eq. (1) holds with equality.

Lemma 1. Any triangle ring network G satisfies Eq. (1). Figure 5 shows a typical subgraph of the type considered in the proof of Lemma 1.

Proof. Suppose the contrary. Then there is a vertex-induced subgraph T on v' vertices that violates Eq. (1). If T contains a vertex v of degree 1 then $T - v$ also violates Eq. (1) so we may assume that T has minimum degree 2. In this case, T has at most two vertices of degree 2, since it has maximum degree 3. In particular, T may be disconnected from G by removing at most two edges. If T is an interior subgraph, we get a contradiction right away. Alternatively, at least one of the degree 2 vertices in T is degree 2 in G, and so on C. If exactly one is, then G is not 2-connected. If both are, then $T = G$ and there are only two boundary vertices. Either case is a contradiction. ■

Corollary 1. The rigid subgraphs of a triangle ring network G are the subgraphs containing exactly three vertices of degree 2 and every other vertex has degree 3. Moreover, any proper rigid subgraph contains at most one boundary vertex of G.

Proof. The first statement is straightforward. The second follows from observing that if a rigid subgraph T has two vertices on the boundary of G then G cannot be 2-connected, since all the edges detaching T from G are incident on a single vertex. ■

When G is planar, these rigid subgraphs are regions cut out by cycles of length 3 in the Poincaré dual. More generally in the planar case, subgraphs corresponding to regions that are smaller triangle ring networks with t degree 2 vertices have t degrees of freedom.

B. Anchoring with sliders

Now we can consider our first anchoring model, which uses *slider pinning* [12]. A *slider* constrains the motion of a point to remain on a fixed line, rigidly attached to the plane. When we talk about attaching sliders to a vertex of the graph, we choose a point on the corresponding triangle, and constrain its motion by the slider. In the results used below, this point should be chosen generically; for example, the theory does not apply if the slider is attached at a pinned corner shared by two of the triangles. Since we are only attaching sliders to triangles corresponding to degree 2 vertices in G, we may always attach sliders at an unpinned triangle corner.

The notion of rigidity for networks of bodies with sliders is that of being *pinned* [25]: the system is completely immobilized [26]. A network with sliders is *pinned-isostatic* if it is pinned, but ceases to be so if any pin or slider is removed.

The equivalent of the White-Whiteley counts in the presence of sliders is a theorem of Katoh and Tanigawa [27], which says that a generic slider-pinned body-pin network G is independent if and only if the body-pin graph satisfies Eq. (1) and

$$2e' + s' \leqslant 3v' \qquad \text{for all subgraphs } G' \subset G, \tag{2}$$

where s' is the number of sliders on vertices of G'. Here is our first anchoring procedure.

Theorem 1. Adding one slider to each degree 2 boundary vertex of a triangle ring network G gives a pinned-isostatic network.

Proof. Let T be an arbitrary subgraph with v' vertices and v'' vertices of degree at most 2. That Eq. (1) holds is Lemma 1. The fact that the only vertices of T which get a slider are vertices with degree 2 in G implies that Eq. (2) is also satisfied, and, by construction $2e + s = 3v$. ■

We may think of this anchoring as rigidly attaching a rigid wire to the plane, then constraining the boundary vertices to move on it. Provided that the wire's path is smooth and sufficiently nondegenerate, this is equivalent, for analyzing infinitesimal motions, to putting the sliders in the direction of the tangent vector at each boundary vertex. See also Fig. 2.

C. Anchoring with immobilized triangle corners

Next, we consider anchoring G by immobilizing (pinning down) some points completely. Combinatorially, we model immobilizing a triangle's corner by adding two sliders through it. Since we are still using sliders, the definitions of pinned and pinned-isostatic are the same as in the previous section.

The analog for Eq. (2) when we add sliders in groups of two is

$$2e' + 2s' \leqslant 3v' \qquad \text{for all subgraphs } G' \subset G, \tag{3}$$

where s' is the number of immobilized corners.

Theorem 2. Let G be a triangle ring network with an even number t of degree 2 vertices on C. Then, following C in cyclic order, pinning every other boundary vertex that is encountered results in a pinned-isostatic network.

Proof. Let T be an arbitrary subgraph of G. If at most one of the vertices of T is pinned, there is nothing to do. For the moment, suppose that no vertex of degree 1 in T is pinned. Let t be the number of pinned vertices in T.

We will show that for each of the t pinned vertices there is a distinct unpinned vertex of degree 1 or 2 in t. This implies that $2e' \leqslant 3v' - 2t$ in T, at which point we know Eq. (3) holds for T.

To prove the claim, let v be a pinned vertex of T. Traverse the boundary cycle C from v. Let w be the next pinned vertex of T that is encountered. If the chain from v to w along C is in T, the alternating pattern provides an unpinned degree 2 vertex that is degree 2 in G. Otherwise, this path leaves T, which can only happen at a vertex with degree 1 or 2 in T. Continuing the process until we return to v produces at least t distinct unpinned degree 2 vertices, since each step considers a disjoint set of vertices of C.

Now assume that T does have a pinned vertex v of degree 1. The theorem will follow if Eq. (3) holds strictly for $T - v$. Let w and x be the pinned vertices in T immediately preceding and following v. The argument above shows that there are at least two unpinned degree 1 or 2 vertices in T on the path in C between w and x on C. Since these are in $T - v$, we are done. ■

When there are an odd number of boundary vertices in G, Theorem 2 does not apply. This next lemma gives a simple reduction in many cases of interest.

Theorem 3. Let G be a planar triangle ring network, with C the outer face. Suppose that there are an odd number t of boundary vertices. If G is not a single cycle, then it is possible to obtain a network with an even number of boundary vertices by removing the intersection of a facial cycle of G with C, unless $G = C$.

Proof sketch. The connectivity requirements for a triangle ring network combined with planarity of G imply that the intersection of C and any facial cycle D of G is a single chain. Every boundary vertex is in the interior of such a chain, so some facial cycle D contributes an odd number of boundary vertices. Removing the edges in $D \cap C$ changes the parity of the number of boundary vertices. ■

D. Anchoring with additional bars

So far, we have worked with networks of triangles pinned together. Now we augment the model to also include bars between pairs of the triangles. We will always take the end points of the bars to be free corners of triangles that are boundary vertices in the underlying network G. Combinatorially we model this by a graph H on the same vertex set as G, with an edge for each bar between a pair of bodies. In this case, the Tay-Whiteley count becomes

$$2e' + b' \leqslant 3v' - 3 \qquad \text{for all subgraphs } G' \subset G, \tag{4}$$

where e' is the number of edges in G' and b' is the number of edges in H spanned by the vertices of G'. The anchoring procedures with sliders or immobilized vertices have analogs in terms of adding bars to create an isostatic network. These boundary conditions are illustrated on the right-hand side of Fig. 6. Also shown in Fig. 6 in the left panel is a triangular scheme involving alternating unpinned surface sites, that is equivalent to anchoring. In both cases shown here the sample is free to rotate with respect to the page.

Theorem 4. If G has boundary vertices $v_1, \ldots, v_t$, we obtain an isostatic framework by taking the edges of H to be $v_1v_2, v_2v_3, \ldots, v_{t-3}v_{t-2}$.

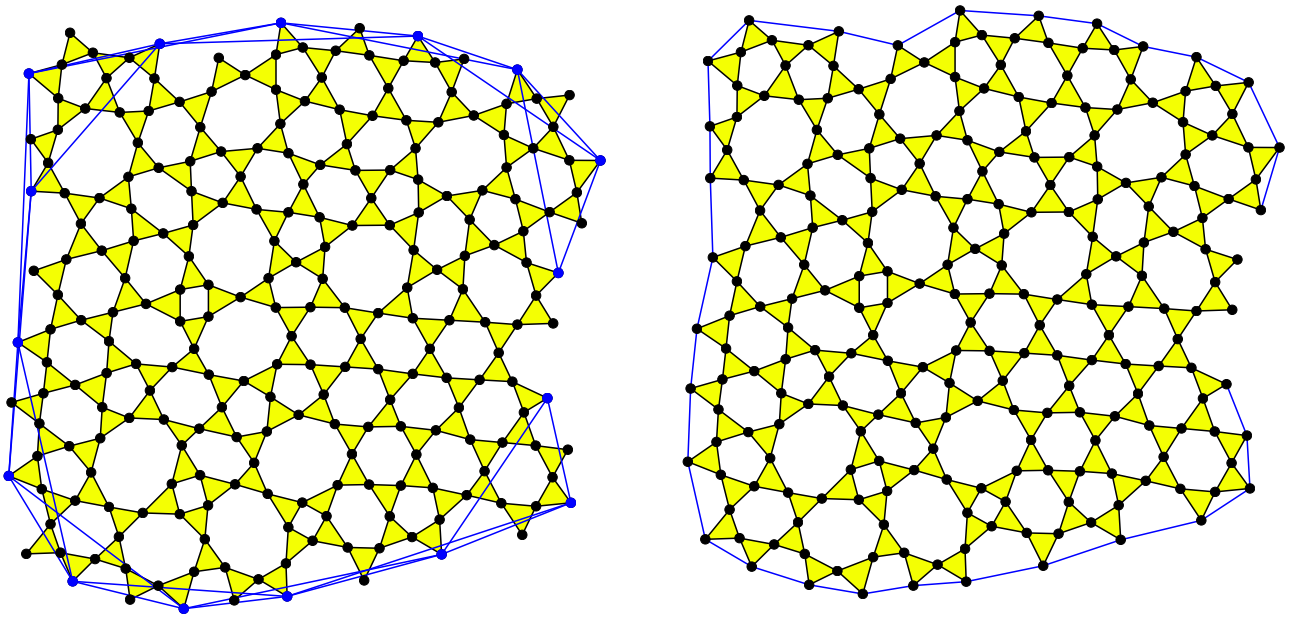

FIG. 6. (Color online) Two additional boundary conditions used for the sample shown in Fig. 3, with the three purple triangles at the lower left removed to give an even number of unpinned surface sites. On the left, alternating surface sites are connected to one another through triangulation of first and second neighbors, with the last three connections not needed (these would lead to redundancy). Hence there are three additional macroscopic motions when compared to Fig. 3 which can be considered as being pinned to the page rather than to the *internal frame* shown by blue straight lines. On the right we illustrate anchoring with additional bars which connect all unpinned surface sites, except again three are absent, to avoid redundancy, and to give the three additional macroscopic motions when compared to Fig. 3.

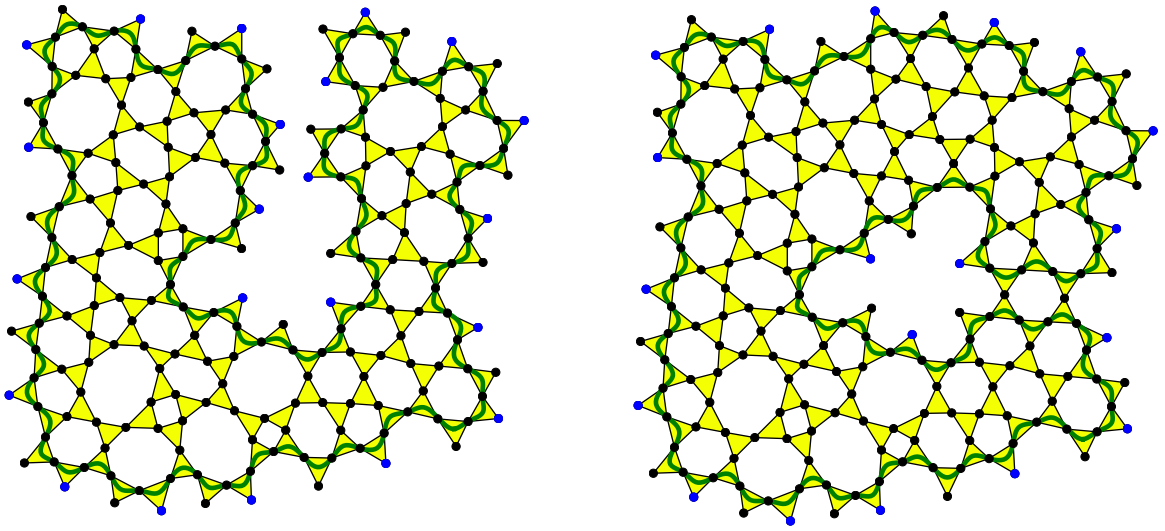

FIG. 7. (Color online) Two, at first sight, more complex anchored boundary conditions that by our results can be used for the sample shown in Fig. 2, with the three purple triangles at the lower left removed to give an even number of unpinned surface sites. The anchored sites are shown as blue discs, with an even number of surface sites in both graphs. The graph at the right has an even number of surface sites in *both* the outer and inner boundary. The red Si atoms at the centers of the triangles have been suppressed for clarity. The green line goes through the boundary triangles.

Proof. Consider the $t-3$ new bars. By construction and Lemma 1 we have $2e+t-3=3v-t+t-3=3v-3$. Corollary 1 and the connectivity hypotheses imply that no rigid subgraph of G has more than one of its three degree 2 vertices on the boundary of G. This shows that no rigid subgraph of G has a bar added to it. ■

Theorem 5. If G has t boundary vertices and t is even, then taking H to be any isostatic bar-joint network with a vertex set consisting of $t/2$ boundary vertices chosen in an alternating pattern around C results in an isostatic network.

A triangulated $t/2$-gon is a simple choice for H.

Proof sketch. By Lemma 1, we are adding enough bars to remove all the internal degrees of freedom. The desired statement then follows from Theorem 2 by observing that pinning down the boundary vertices is equivalent, geometrically, to pinning down H and then identifying the boundary vertices of G to the vertices of H. ■

A result of White and Whiteley [28] on "tie downs" then gives the following.

Corollary 2. In the situation of Theorems 4 and 5, adding *any* three sliders results in a pinned-isostatic network.

E. Stressed regions

So far, we have shown how to render a floppy triangle ring network isostatic or pinned-isostatic. It is interesting to know when adding a single extra bar or slider results in a network that is stressed over all its members. This is a somewhat subtle question when adding bars or immobilizing vertices, but it has a simple answer for the sliding boundary conditions.

We say that a triangle ring network is *irreducible* if (a) every minimal two edge cut set either detaches a single vertex from G or both remaining components contain more than one boundary vertex of G or (b) every minimal three edge cut set disconnects one vertex from G.

Lemma 2. A triangle ring network G has no proper rigid subgraphs if and only if G is irreducible.

Proof. Recall, from Corollary 1, that a proper rigid subgraph T of G has exactly three vertices of degree 2 and the rest degree 3. Thus, T can be disconnected from G by a cut set of size 2 or 3.

In the former case, Corollary 1 implies that exactly one of the degree 2 vertices in T is a boundary vertex of G. This means that T witnesses the failure of (a), and G is not irreducible. Conversely, (a) implies that, for a two edge cut set not disconnecting one vertex, either side is either a chain of boundary vertices or has at least four vertices of degree 2.

Finally, observe that cut sets of size 3 are minimal if and only if they disconnect an interior subgraph on one side. Corollary 1 then implies that there is a proper rigid component that is an interior subgraph of G if and only if (b) fails. ■

Theorem 6. Let G be a triangle ring network anchored using the procedure of Theorem 1. Adding *any* bar or slider to G results in a network with all its members stressed if and only if G is irreducible.

Proof. First consider adding a slider. Because G is pinned-isostatic, the slider creates a unique stressed subgraph T. A result of Streinu and Theran [12] implies that T must have been fully pinned in G. Since any proper subgraph has an unpinned vertex of degree 1 or 2, Eq. (2) holds strictly. Thus, the stressed graph is all of G [29]. If we add a bar, there is also a unique stressed subgraph. This will be all of G, again using [12], unless both end points of the bar are in a common rigid subgraph. That was ruled out by assuming that G is irreducible. ■

III. CONCLUSIONS

In this paper we have demonstrated boundary conditions for locally isostatic networks that incorporate the right number of constraints at the surface so that the whole network is isostatic.

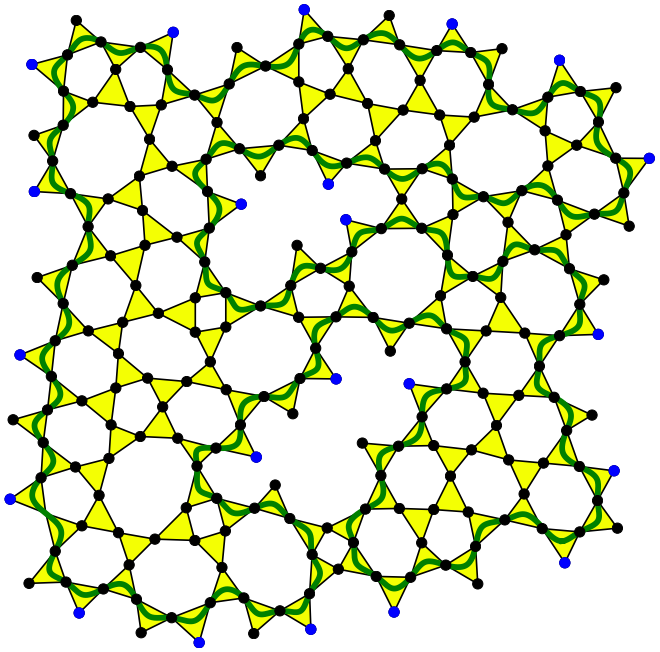

FIG. 8. (Color online) Even more complex boundaries, developed from the sample shown in Fig. 3 by removing triangles to form two internal *holes*. The boundary sites are shown as blue discs and the three purple triangles at the lower left in Fig. 3 have been removed. The red Si atoms at the centers of the triangles in Fig. 1 have also been removed for clarity. The green line forms a continuous *boundary* which goes through all the surface sites which must be an even number. The anchored (blue) sites then alternate with the unpinned sites on the green boundary curve which has to cross the bulk sample in two places to reach the two internal holes. Here there are 32 boundary sites, 5 boundary sites in the upper hole and 7 in the lower hole, giving a total even number of 44 boundary sites. Where these crossings take place is arbitrary, but it is important that the anchored and unpinned surface sites alternate along whatever (green) boundary line is drawn.

These boundary conditions should be useful in numerical simulations which involve finite pieces of locally isostatic networks. The boundary can be quite complex and involve both an external boundary with internal holes.

Our derivation of the new boundary conditions is based on a structural characterization of graphs which capture the combinatorics of silica bilayers. This shows that the degrees of freedom are associated with unpinned triangle corners on the boundary. We then present two methods to completely immobilize a triangle ring network: by attaching the boundary to a wire rigidly attached to the plane, and by completely immobilizing alternate vertices on the boundary. To render a triangle ring network isostatic, we also have two methods: adding bars between adjacent boundary vertices in cyclic order and attaching alternating boundary vertices to an auxiliary graph that functions as a rigid frame.

Although our definition of a triangle ring network is most easily visualized when G is planar and C is the outer face, the combinatorial setup is quite a bit more general. The natural setting for networks with holes is to assume planarity, and then to assume that all the degree 2 vertices are on disjoint facial cycles in G. The key thing to note is that the cycle C in our definition does not need to be facial for Theorem 2. For example, in Fig. 7, C goes around the boundary of an interior face that contains degree 2 vertices. In general, the existence of an appropriate cycle C is a nontrivial question, as indicated by Fig. 7 (see also Fig. 8 for another, more complicated, example of anchored boundary conditions).

What is perhaps more striking is that Theorem 1 still applies whether or not such a C exists, provided faces in G defining the holes in the sample are disjoint from the boundary and each other.

In applying anchored boundary conditions, it is important that the complete boundary has an even number of unpinned sites, which can include internal holes, which must then be connected using the green lines shown in the various figures. This gives a practical way of setting up calculations with anchored boundary conditions in samples with complex geometries and missing areas.

ACKNOWLEDGMENTS

Support by the Finnish Academy (AKA) Project COALESCE is acknowledged by L.T. We thank Mark Wilson and Bryan Chen for many useful discussions and comments. This work was initiated at the American Institute of Mathematics (AIM) workshop on configuration spaces, and we thank AIM for its hospitality.

APPENDIX: IMPLEMENTATION DETAILS

Algorithms 1–4 in this appendix give a procedural description of the four boundary conditions discussed in this paper, and make clear the subtle differences between them. All of the algorithms in this appendix take as input a finite part of a locally isostatic network and output a globally isostatic one that is appropriate for further study. Which of the boundary conditions is most appropriate will depend on the intended application.

Before describing the algorithms, we give more detail on how to encode a triangle ring network and the associated set of first-order geometric constraints.

1. Encodings

Computationally, it is convenient to work not only with the body graph G, as in the main body of the paper, but also with its *line graph* G^* that has as its vertices the triangle corners and edges the triangle sides. We denote by n and m the number of vertices and edges in G, and we denote by n^* and m^* the same quantities for G^*. Vertices in G are denoted by $v, w, \ldots$ and vertices in G^* are denoted by $v^*, w^*, \ldots$. We assume that there is a constant-time mapping $\tau : V(G) \to V(G^*)^3$ that maps each vertex v of G to the associated triangle $\{v_v^*, w_v^*, x_v^*\}$ in G^*. For each boundary vertex v of G, $\tau(v)$ will have a unique degree 2 vertex, which we denote by $T(v)$.

Experimentally, G^* will always be immediately visible. It is also computable in time $O(n)$ from G. If G is planar with given facial structure [30], then G^* also has a natural planar embedding, and vice versa. Further, if G^* contains no pair of facial triangles with a common edge, then G is determined by G^*. This is the case in all of our examples.

We also assume that we have access to the coordinates of the vertices of G^*. We denote these by $p(v^*) = (x_{v^*}, y_{v^*})$ for each vertex v^* of G^* and call p a *placement*.

2. First-order geometric constraints

The allowed first-order motions $\dot{p}$ of a triangle ring network G satisfy the system

$$\langle p(v^*) - p(w^*), \dot{p}(v^*) - \dot{p}(w^*)\rangle = 0 \quad \text{for all edges } v^*w^* \in E(G^*). \tag{A1}$$

We assume that p maximizes the rank of Eq. (A1), which happens for almost all choices of p. By the theorems in this paper, this rank is equal to m^* when G is a triangle ring network.

Now identify a set $S^* \subset V(G^*)$ of vertices to which we will add one slider constraint. Assign a vector $s(v^*) = (a_{v^*}, b_{v^*})$ to each $v^* \in S^*$. The slider constraints on the first-order motions are

$$\langle s(v^*), \dot{p}(v^*)\rangle = 0 \quad \text{for all } v^* \in S^*. \tag{A2}$$

To guarantee that the combined system (A1) and (A2) achieves its maximum rank ($2n^*$ for our sliding boundary condition), it is sufficient to pick each $s(v^*)$ uniformly at random from the unit circle [32].

3. Implementing slider pinning

Algorithm 1 shows how to implement the sliding boundary condition of Theorem 1. (See Fig. 2.)

Algorithm 1 Sliding boundary conditions.
Input: Triangle ring network G, line graph G^*.
Output: Slider constraints implementing the sliding boundary condition.
1: Initialize S^* to the empty set.
2: For each boundary vertex v of G, add $T(v)$ to S^*.
3: For each v^* in S^*, generate a random vector $s(v^*)$ on the unit circle, and use it to create a slider constraint of the form (A2).

4. Implementing immobilized vertices

To implement Theorem 2 (see Figs. 3 and 7), we could put two independent sliders at vertices of G^*. However, it is simpler to regard Eq. (A1) as a matrix and then discard the columns corresponding to immobilized vertices.

Algorithm 2 Pinned boundary conditions.
Input: Triangle ring network G with an even number of boundary vertices, line graph G^*, boundary cycle C.
Output: Linear constraints pinning (A1).
1: Let M be the matrix of the system (A1).
2: Pick a vertex v_0 on C. Set $v = v_0$. Set $b = 1$.
3: If $b = 1$, discard the columns in M corresponding to $T(v)$, and set $b = 0$. Otherwise set $b = 1$. Replace v with its successor on C.
4: If $v = v_0$, output M. Otherwise, go to step 3.

Observe that the loop implemented in steps 2–4 shows how to obtain the free corners of the boundary vertices of G.

5. Implementing anchoring with additional bars

Anchoring with additional bars amounts to adding edges to G^*. (See Fig. 6.) Thus, we describe the graph theoretically only. If the geometric constraints are desired, simply use the new graph to write down Eq. (A1).

Algorithm 3 Anchoring with bars I.
Input: Triangle ring network G, line graph G^*, boundary cycle C.
Output: An isostatic graph containing G^*.
1: Enumerate the boundary vertices $v_1, \ldots, v_t$ of G, ordered along C.
2: Set $H = G^*$.
3: Add edges $T(v_1)T(v_2), \ldots, T(v_3)T(v_2)$ to H.
4: Output H.

The left panel of Fig. 6 takes the graph H from Theorem 5 to be a "zig-zag triangulation" of a polygon, which is easily seen to be isostatic. This next algorithm gives the implementation of Theorem 5 using this choice.

Algorithm 4 Anchoring with bars II.
Input: Triangle ring network G with an even number of boundary vertices, line graph G^*, boundary cycle C.
Output: An isostatic graph containing G^*.
1: Enumerate alternating boundary vertices $v_1, v_3, \ldots, v_t - 1$ of G, ordered along C.
2: Set $H = G^*$.
3: Add edges $T(v_1)T(v_3), T(v_3)T(v_5), T(v_1)T(v_5)$ to H.
4: For $i = 7, 9, \ldots, t - 1$, add the edges $T(v_{i-2})T(v_i), T(v_{i-4})T(v_i)$ to H.
5: Output H.

[1] O. Hod, J. E. Peralta, and G. E. Scuseria, Edge effects in finite elongated graphene nanoribbons, Phys. Rev. B **76**, 233401 (2007).

[2] M. F. Thorpe, Bulk and surface floppy modes, J. Non-Cryst. Solids **182**, 135 (1995).

[3] T. C. Lubensky, C. L. Kane, X. Mao, A. Souslov, and K. Sun, Phonons and elasticity in critically coordinated lattices, Rep. Prog. Phys. **78**, 073901 (2015).

[4] W. G. Ellenbroek, V. F. Hagh, A. Kumar, M. F. Thorpe, and M. van Hecke, Rigidity Loss in Disordered Systems: Three Scenarios, Phys. Rev. Lett. **114**, 135501 (2015).

[5] L. Lichtenstein, C. Büchner, B. Yang, S. Shaikhutdinov, M. Heyde, M. Sierka, R. Włodarczyk, J. Sauer, and H.-J. Freund, The atomic structure of a metal-supported vitreous thin silica film, Angewandte Chemie International Edition **51**, 404 (2012).

[6] M. Wilson, A. Kumar, D. Sherrington, and M. F. Thorpe, Modeling vitreous silica bilayers, Phys. Rev. B **87**, 214108 (2013).
[7] A. Kumar, D. Sherrington, M. Wilson, and M. F. Thorpe, Ring statistics of silica bilayers, J. Phys.: Condens. Matter **26**, 395401 (2014).
[8] G. Laman, On graphs and rigidity of plane skeletal structures, J. Engrg. Math. **4**, 331 (1970).
[9] D. J. Jacobs and M. F. Thorpe, Generic Rigidity Percolation: The Pebble Game, Phys. Rev. Lett. **75**, 4051 (1995).
[10] D. J. Jacobs and M. F. Thorpe, Generic rigidity percolation in two dimensions, Phys. Rev. E **53**, 3682 (1996).
[11] M. Sadjadi, M. Wilson, and M. F. Thorpe, Computer refinement of experimentally determined structures at the atomic level (to be published).
[12] I. Streinu and L. Theran, Slider-pinning rigidity: A Maxwell-Laman-type theorem, Discrete Comput. Geom. **44**, 812 (2010).
[13] See, e.g., the monograph by Graver *et al.* [14] for an introduction.
[14] J. Graver, B. Servatius, and H. Servatius, *Combinatorial Rigidity*, Vol. 2 (American Mathematical Society, Providence, RI, 1993), p. 172.
[15] J. C. Maxwell, On the calculation of the equilibrium and stiffness of frames, London, Edinburgh, and Dublin Philosophical Magazine and Journal of Science **27**, 294 (1864).
[16] To make this paper somewhat self-contained, we will briefly explain the concepts we use. Our terminology is standard and can be found in, e.g., the textbook by Bondy and Murty [17].
[17] J. A. Bondy and U. S. R. Murty, *Graph Theory*, Vol. 244 (Springer, New York, 2008).
[18] Since only two triangles are pinned together at any point, we are dealing with the two-dimensional specialization of body-hinge frameworks first studied by Tay [19] and Whiteley [20] in general dimensions. In two dimensions, there is a richer combinatorial theory of "body-multipin" structures, introduced by Whiteley [21]. See Jackson and Jordán [22] and the references therein for an overview of the area.
[19] T.-S. Tay, Linking $(n-2)$-dimensional panels in n-space. II. $(n-2,2)$-frameworks and body and hinge structures, Graphs Combin. **5**, 245 (1989).
[20] W. Whiteley, The union of matroids and the rigidity of frameworks, SIAM J. Discrete Math. **1**, 237 (1988).
[21] W. Whiteley, A matroid on hypergraphs, with applications in scene analysis and geometry, Discrete Comput. Geom. **4**, 75 (1989).
[22] B. Jackson and T. Jordán, Pin-Collinear Body-and-Pin Frameworks and the Molecular Conjecture, Discrete and Computational Geometry **40**, 258 (2008).
[23] This means that to disconnect G we need to remove at least two vertices.
[24] This is an inclusionwise minimal set of edges that, when removed from G, results in a graph of two connected components.
[25] This terminology, which is from [12], should not be confused with the pins (or pin joints) holding adjacent triangles together.
[26] Rigid body motions are not "trivial," because slider constraints are not preserved by them.
[27] N. Katoh and S.-i. Tanigawa, Rooted-tree decompositions with matroid constraints and the infinitesimal rigidity of frameworks with boundaries, SIAM J. Discrete Math. **27**, 155 (2013).
[28] N. L. White and W. Whiteley, The algebraic geometry of stresses in frameworks, SIAM J. Algebraic Discrete Methods **4**, 481 (1983).
[29] It is worth noting that, so far, irreducibility of G was not required. It is needed only for adding bars.
[30] For example, given as a doubly connected edge list. See, e.g., Sec. 2.2 of the textbook by de Berg *et al.* [31] .
[31] M. de Berg, O. Cheong, M. van Kreveld, and M. Overmars, *Computational Geometry*, 3rd ed. (Springer-Verlag, Berlin, 2008), p. 386, algorithms and applications.
[32] See the appendix of Király *et al.* [33] for a detailed justification of this and similar statements relating genericity and random sampling.
[33] F. J. Király, R. Tomioka, and L. Theran, The algebraic combinatorial approach for Low-Rank Matrix Completion, JMLR **16**, 1391 (2015).